Nuclear Engineering and Design 239 (2009) 2778–2785

Contents lists available at ScienceDirect

Nuclear Engineering and Design

journal homepage: www.elsevier.com/locate/nucengdes

Development of a safety analysis code for molten salt reactors

Dalin Zhang[a,b], Suizheng Qiu[a,b,*], Guanghui Su[a,b]

[a] State Key Laboratory of Multiphase Flow in Power Engineering, Xi'an Jiaotong University, 28 West Road Xian Ning Street, Xi'an 710049, PR China
[b] School of Nuclear Science and Technology, Xi'an Jiaotong University, 28 West Road Xian Ning Street, Xi'an 710049, PR China

ARTICLE INFO

Article history:
Received 2 March 2009
Received in revised form 21 August 2009
Accepted 31 August 2009

ABSTRACT

The molten salt reactor (MSR) well suited to fulfill the criteria defined by the Generation IV International Forum (GIF) is presently revisited all around the world because of different attractive features of current renewed relevance. The MSRs are characterized by using the fluid-fuel, so that their technologies are fundamentally different from those used in the conventional solid-fuel reactors. In this work, in particular, the attention is focused on the safety characteristic analysis of the MSRs, in which a point kinetic model considering the flow effects of the fuel salt is established for the MSRs and calculated by developing a microcomputer code coupling with a simplified heat transfer model in the core. The founded models and developed code are applied to analyze the safety characteristics of the molten salt actinide recycler and transmuter system (MOSART) by simulating three types of basic transient conditions including the unprotected loss of flow, unprotected overcooling accident and unprotected transient overpower. Some reasonable results are obtained for the MOSART, which show that the MOSART conceptual design is an inherently stable reactor design. The present study provides some valuable information for the research and design of the new generation MSRs.

1. Introduction

The MSR concept was first proposed by Oak Ridge National Laboratory (ORNL), and had been researched and developed extensively in their projects of the aircraft reactor experiment (ARE) and the molten salt reactor experiment (MSRE) from 1940s to 1960s (Bettis et al., 1957; Rosenthal et al., 1970). These two projects established the basic technologies for the MSR, and demonstrated its main advantages, including good neutron economy, inherent safety and on-line refueling, processing and fission product removal.

These advantages make MSR attractive also for the present Generation IV International Forum, and being one of the six candidates for the Generation IV Reactor. Therefore, worldwide research activities are being conducted to study and develop new concept MSRs for different attractive features of current renewed relevance. Some new MSR concepts have been proposed, such as the small molten salt reactor (SMSR) (Mitachi et al., 1995), the actinides molten salt transmuter (AMSTER) (MOST Project, 2004), MOSART (Ignatiev et al., 2006) and thorium molten salt reactor (TMSR) (Merle-Lucotte et al., 2008).

Many studies have been conducted on different fields for different MSR concepts. Yamamoto et al. (2005) performed the steady state analysis for the SMSR coupling the neutron diffusion equations with the heat transfer equations in fuel salt and graphite. Krepel et al. (2005, 2007) developed the DYN1D-MSR and DYN3D-MSR codes for MSRs with ORNL's concepts. Wang et al. (2006) focused on the fluid dynamic simulations and optimizations of the MOSART core with the code SIMMER-III by extending the thermo-hydraulic and neutronic models. However, the safety characteristic studies found in open literatures mainly focus on the molten salt breeder reactor (MSBR) and SMSR by Shimazu (1978a,b) and Suzuki and Shimazu (2006, 2008).

In order to provide more basic understanding of the safety characteristics of the MSRs, in the present study, a general point kinetics model considering the flow effect of the fuel salt is founded for the fluid-fuel reactors. This model is solved by developing a microcomputer code coupling with a simplified heat transfer mechanism in the core. We apply this code to analyze the safety characteristics of the MOSART conceptual design that was developed for burning spent nuclear fuel. Three types of basic transient conditions including unprotected loss of flow (ULOF), unprotected overcooling accident (UOC), and unprotected transient overpower (UTOP) are analyzed for the MOSART. And the relative power, temperatures of the fuel salt and the graphite, and the temperature feedback reactivity changing with time are obtained.

2. Physical models and solution method

2.1. Core power model

Point kinetics model with six families of delayed neutron is generally adopted for the solution of the core power in safety analysis.

* Corresponding author at: School of Nuclear Science and Technology, Xi'an Jiaotong University, 28 West Road Xian Ning Street, Xi'an 710049, PR China.
E-mail address: szqiu@mail.xjtu.edu.cn (S. Qiu).

0029-5493/$ – see front matter © 2009 Elsevier B.V. All rights reserved.
doi:10.1016/j.nucengdes.2009.08.020

Nomenclature

t	time
M	mass
T	temperature
n	neutron density
C_p	specific heat
P_r	reactor power
Nu	Nusselt number
Pr	Prandtl number
Re	Reynolds number
w	mass flow rate of fluid-fuel
c_i	delayed neutron precursor concentration of family i
A_{fg}	heat transfer area between the fuel salt and graphite
h_{fg}	heat transfer coefficient between fuel salt and graphite
F	fraction of the fission heat released in fuel salt or graphite
V	Fuel salt volume in the core or external loop

Greek symbols

μ	viscosity
ρ	reactivity
$\tilde{\beta}_{eff}$	effective fraction of delayed neutrons
Λ	neutron generation lifetime
λ_i	precursor decay constant of family i
β_i	precursor fraction of family i
τ	residence time of precursors in the core or external loop
α	reactivity coefficient of the fuel slat or graphite

Superscripts/subscripts

c	the reactor core
l	the external loop
f	fuel salt
g	graphite
in	inlet
out	outlet
av	average

However, the flow effects of the fuel salt in the fluid-fuel reactors render the conventional point kinetics equations for the solid-fuel reactors not available.

Several modeling options for accounting the flow effects are described in the field of reactor safety analyses. The simplest option (Merle-Lucotte et al., 2008) is to only modify the original effective delayed neutron fraction β_{eff} by $\tilde{\beta}_{eff}$ in the conventional point kinetics equations, while the equations for the effective delayed neutron precursors are the same as those for solid-fuel reactors. A more complex model (Suzuki and Shimazu, 2008) leads to modification of the calculating procedure for computing effective delayed neutron precursors $c_i(t)$, in which equations for the effective precursors are modified in order to account explicitly for their decay out of the core. Rineiski et al. (2005) proposed a general model, in which the spatial distribution of the precursors is modeled and then the effective precursors (employed in the point kinetics part that serves for accelerating spatial kinetics calculations) are computed by averaging these spatial distributions while using the adjoint neutron flux as weighting function. Zhang et al. (2009) compare the three mentioned models based on the analysis of the MOSART conceptual design, and find that the results calculated by different models show the similar behavior.

In this study, a new simple point kinetics model is developed and established based on the above general model for the fluid-fuel reactors, in which modification are conducted both on the equations for the neutron density and also especially for the delayed neutron precursors. In the neutron density equation, the effective delayed neutron fraction β_{eff} is replaced by $\tilde{\beta}_{eff}$ and also introducing the loss of delayed fraction β_{loss} varying with the flow change. The delayed neutron precursors are split into two components: ones in the reactor core presented by $c_{c,i}$ (i denotes the family of the delayed neutron precursors), and the others in the external loop by $c_{l,i}$, in which only $c_{c,i}$ has contribution to the neutron density. The reactor kinetics equations for the fluid-fuel reactors take the following form:

$$\frac{dn(t)}{dt} = \frac{\rho(t) - \tilde{\beta}_{eff}}{\Lambda} n(t) + \sum_{i=1}^{6} \lambda_i c_{c,i} \tag{1}$$

$$\frac{dc_{c,i}}{dt} = \frac{\beta_i}{\Lambda} n(t) - \lambda_i c_{c,i} + c_{l,i} \frac{1}{\tau_l} \left(\frac{V_l}{V_c} \right) - c_{c,i} \frac{1}{\tau_c} \tag{2}$$

$$\frac{dc_{l,i}}{dt} = -\lambda_i c_{l,i} + c_{c,i} \frac{1}{\tau_c} \left(\frac{V_c}{V_l} \right) - c_{l,i} \frac{1}{\tau_l} \tag{3}$$

where $\tau_c = M_c/w(t)$; $\tau_l = M_l/w(t)$; and $\tilde{\beta}_{eff} = \beta_{static} - \beta_{loss}$. The third and second term on the right side of Eqs. (2) and (3) indicate the delayed neutron precursors flowing into the core and the external loop, while the last terms indicate those flowing out the core and the external loop, respectively.

2.2. Heat transfer model in the core

The simplified heat transfer model in the core is founded for the fuel salt and the graphite based on the energy conservation principle, respectively, which will be calculated coupling with the reactor power model:

$$M_f C_{p,f} \frac{dT_f}{dt} = F_f P_r - 2w(t) C_{p,f} (T_f - T_{in}) + h_{fg} A_{fg} (T_g - T_f) \tag{4}$$

$$M_g C_{p,g} \frac{dT_g}{dt} = F_g P_r + h_{fg} A_{fg} (T_f - T_g) \tag{5}$$

In the calculation, the reactor core is generally divided into some small control volumes along the axial direction. And Eqs. (4) and (5) are applied to every control volume. The average temperature of the fuel salt and the graphite in the core can be calculated with the mass as weighted parameter:

$$T_{f,av} = \frac{\sum M_{f,i} T_{f,i}}{\sum M_{f,i}} \tag{6}$$

$$T_{g,av} = \frac{\sum M_{g,i} T_{g,i}}{\sum M_{g,i}} \tag{7}$$

where the subscript i denotes the number of the control volume. And it is noted that the inlet temperature of the control volume i is the outlet temperature of the control volume $(i-1)$ in flow direction.

2.3. Heat transfer coefficient and temperature reactivity feedback

The calculation of the heat transfer coefficient between the fuel salt and graphite is based on the correlation for the Nusselt number. In order to obtain a realistic result, the molten salt specific correlation for the Nusselt number is adopted, which is proposed by Cox based on actual experimental data generated by ORNL using MSBR salt:

$$Nu = 0.089(Re^{2/3} - 125) Pr^{0.33} \left(\frac{\mu_{bulk}}{\mu_{surf}} \right)^{0.14} \tag{8}$$

where μ_{bulk} is the viscosity at the bulk temperature, and μ_{surf} is that at the surface temperature. In this calculation the fuel salt temperature is used as the bulk temperature, while the graphite temperature is as the surface temperature.

The reactivity feedback caused by the temperature (labeled by subscript T) changes of the fuel salt and the graphite reflector is specially considered:

$$\rho_T(t) = \alpha_f \frac{\sum M_{f,i}(T_{f,i} - T_{f0,i})}{\sum M_{f,i}} + \alpha_g \frac{\sum M_{g,i}(T_{g,i} - T_{g0,i})}{\sum M_{g,i}} \quad (9)$$

where subscript i denotes the number of the control volume in the calculation; and subscript 0 presents the parameter at the rated state.

2.4. Solution method

For the initial steady state conditions, the rated power is given to the neutron density. The initial delayed neutron precursors in the core and in the loop, and the temperatures in the fuel salt and graphite can be obtained by Eqs. (2)–(5) with the time-dependent terms being set to zero.

The transient characteristics of the reactor at a given initial steady state are obtained by solving the set of non-linear ordinary differential equations with different perturbation conditions, such as the loss of flow, the overcooling at the inlet, and the overpower. The set of ordinary differential equations founded for the fluid-fuel reactors can be written as

$$\frac{d\vec{y}}{dt} = f(t, \vec{y}, \vec{y}', x) \quad (10)$$

$$\vec{y}(t_0) = \vec{y}_0 \quad (11)$$

where $\vec{y}$ is the state vector for the calculated variables, such as the neutron density, the precursors concentrations and the temperatures.

We applied the Gear method (Gear, 1971) equipped with Adams predictor–corrector method, which designed especially for stiff equation system to solve the set of equations.

3. Results and discussion

The theoretical models and the solution method have been coded in modular structure and applied to the MOSART, which can be easily modified to be competent for the calculations under different transient conditions of the MOSART even other kinds of MSRs or fluid-fuel reactors. In this work, three types of basic transients, including the unprotected loss of flow (ULOF), unprotected over cooling (UOC), and unprotected transient overpower (UTOP) are analyzed.

3.1. General description of the MOSART concept

The MOSART concept is proposed by RRC-KI, and studied within the coordinated research project (CRP) framework of IAEA to examine and demonstrate the feasibility of molten salt reactors to reduce long lived waste toxicity and to produce efficiently electricity in closed cycle. The MOSART fuel circuit and reactor configuration are represented in the references (Ignatiev et al., 2006; Maschek et al., 2008). Here, the reactor configuration is displayed in Fig. 1, and the basic parameters are listed in Table 1.

3.2. Analysis of unprotected loss of flow (ULOF)

Presuming that the ULOF is initiated by the loss of forced circulations in primary system due to pump failure, in which the mass flow rate decreases to 4% of the rated flow in 7 s as shown in Fig. 2 by the circle symbols, and the inlet temperature of the fuel salt keeps constant (see the triangle symbols in Fig. 3) in calculation.

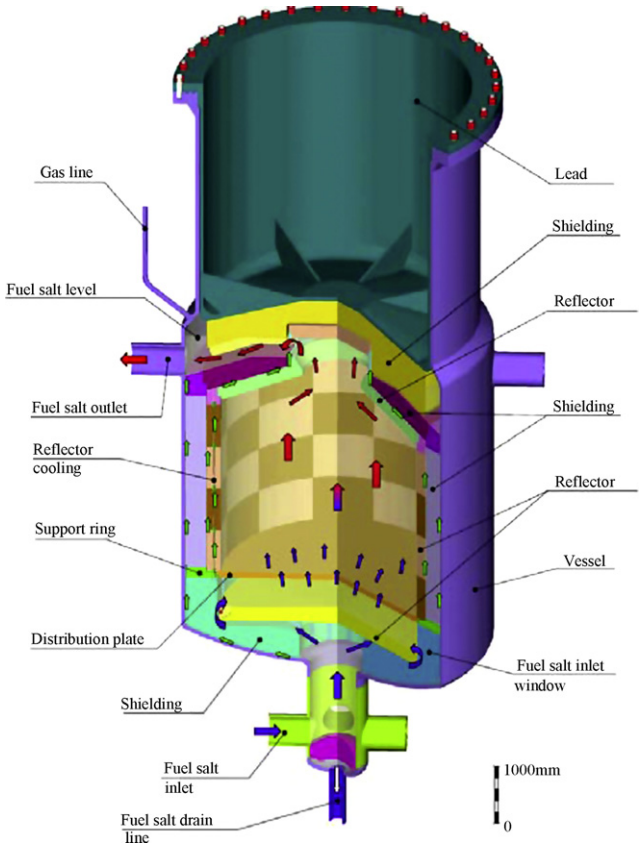

Fig. 1. Reactor configuration of the MOSART.

The loss of flow results in two effects. The first effect is the reduction of the loss of delayed neutrons from the core, which introduces about 82.9 pcm insertion of positive reactivity. The second effect is the increase of the temperatures in the core. Fig. 3 displays the temperatures of the fuel salt and the graphite changing with time, from which, it can be observed that both fuel average and fuel outlet temperatures rise rapidly to about 740 °C and 870 °C at about 40 s into the transient, while the average temperature of the graphite increase a little because of its thermal inertia. The temperatures increase generates strong negative reactivity insertion because of the negative reactivity coefficients of the fuel salt and the graphite. Fig. 4 shows the reactivity feedback caused by the temperatures of the fuel salt and the graphite, from which it can be seen that the reactivity caused by the increase of the fuel salt temperature quickly decreases to the minimum value, while that caused by the

Table 1
Basic parameters of the MOSART.

Parameters	Values
Core diameter/height (m)	3.4/3.6
Core nuclear power (MW)	2,400
Core salt mass flow rate (kg/s)	10,000
Fuel salt mass in the core (kg)	69,914
Fuel salt mass in the external loop (kg)	39,376
Graphite mass in the core (kg)	20,000
Fuel salt volume in the core (m^3)	32.67
Fuel salt volume in the external loop (m^3)	18.4
Core inlet temperature (°C)	600
Core outlet temperature (°C)	715
Graphite temperature (°C)	770
Reactivity coefficient of the fuel temperature (pcm/K)	−4.125
Reactivity coefficient of the graphite temperature (pcm/K)	−0.04

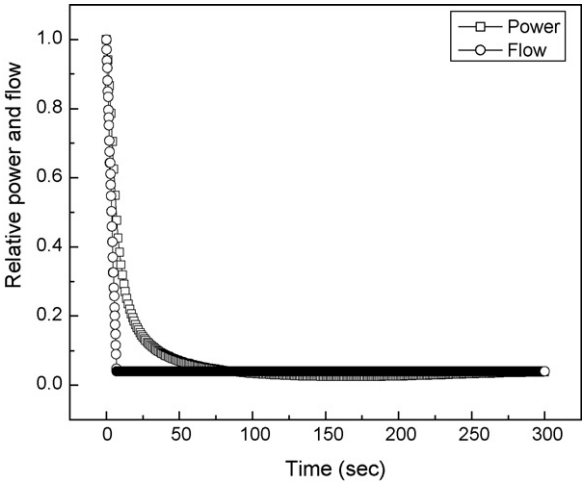

Fig. 2. Relative power and flow in the ULOF.

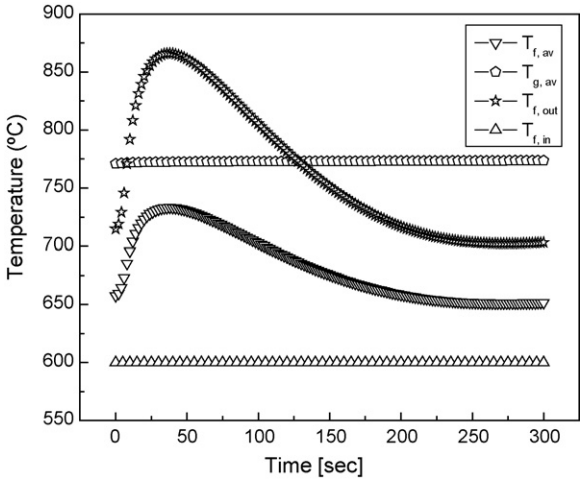

Fig. 3. Temperatures in the ULOF.

graphite temperature decreases little, therefore, the total reactivity caused by the temperatures mainly dependent on the temperature of the fuel salt. The rapid negative reactivity feedback by the temperatures increase balances the positive reactivity insertion by the loss of flow, the net effect of which is a fast decrease in the power

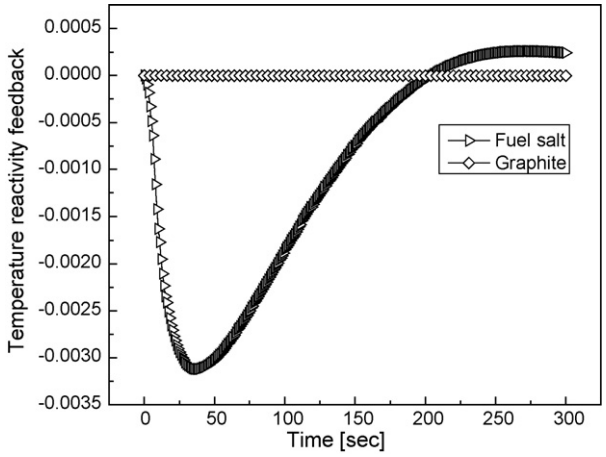

Fig. 4. Temperature reactivity feedback in the ULOF.

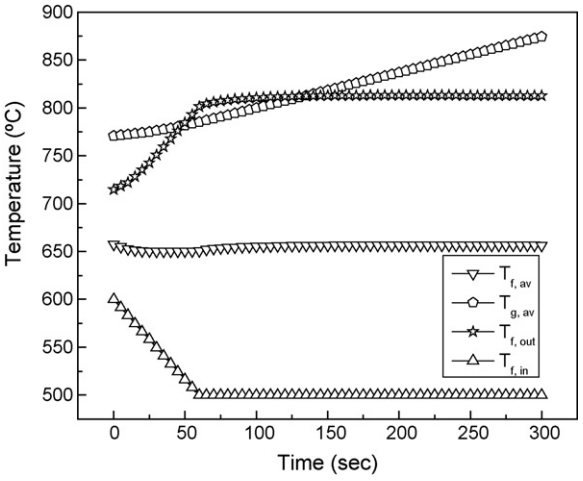

Fig. 5. Temperatures in the UOC.

level to that of the flow drop. Fig. 2 displays the relative power by the square symbols. The power decrease makes the temperature of the fuel salt in the core decreases and stabilizes to near the initial level, and the reactivity increases correspondingly.

3.3. Analysis of unprotected overcooling accident (UOC)

In this case, the inlet temperature of the fuel salt is postulated to decrease 100 °C in 60 s (see triangle symbols in Fig. 5) to simulate the UOC accident, and the mass flow remains constant as shown in Fig. 6 by circle symbols.

The inlet temperature decrease leads to a little decrease of the average temperature of the fuel salt whereas the outlet temperature of the fuel salt increases from 720 °C to 820 °C, which are displayed in Fig. 6. Because the reactivity coefficient of the fuel salt is negative, a positive reactivity feedback caused by the fuel salt is introduced into the reactor as shown in Fig. 7, which results in the power increasing to 2.7 times of its rated value as shown in Fig. 5. From Fig. 6, it also can be found that the average graphite temperature increases gradually, which inserts negative reactivity feedback to balance the positive reactivity introduced by the fuel salt leading to the power and the fuel salt temperature stabilized.

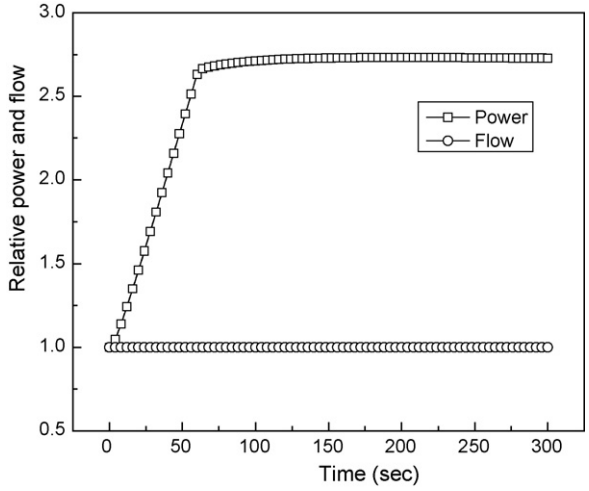

Fig. 6. Relative power and flow in the UOC.

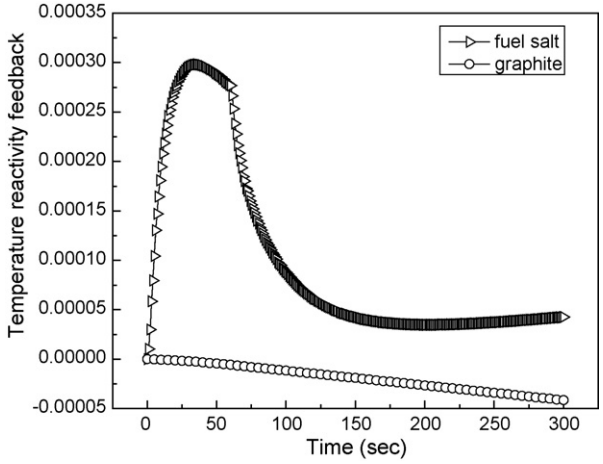

Fig. 7. Temperature reactivity feedback in the UOC.

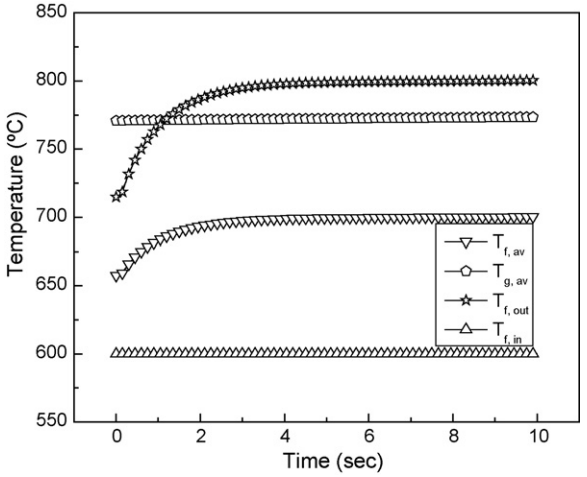

Fig. 9. Temperatures in the UTOP with +200 pcm jump.

3.4. Analysis of unprotected transient overpower (UTOP)

In MSRs, the fuels are generally dissolved in the molten salts to be fluid phase. If the agglomerated fuels are poured into the reactor (which can stay in the core (called reactivity jump), or cycle in the primary loop (called reactivity cycle)), the positive reactivity will be introduced directly and leads to overpower transients.

In the first calculated case of UTOP, +200 pcm (about 60 cent) reactivity of the fuel agglomeration is assumed to be added into the core by a step. The flow and the inlet temperature remain the nominal values in the calculation as shown in Figs. 8 and 9.

The relative power, temperatures and reactivity feedback caused by temperatures are shown in Figs. 8–10, respectively. From Fig. 8, it can be found that a power pulse of about 4 times of the nominal power is generated in short time because of the positive reactivity insertion. Correspondingly, the temperatures of the fuel salt raise quickly, which leads negative reactivity feedback adding into the core fast. Therefore, the power decreases to 1.7 times of the nominal value, and the average temperature and the outlet temperature of the fuel salt stabilizes at 700 °C and 800 °C after increasing in the initial phase. Concurrent with the initial fast increase of the fuel salt temperature, the average temperature of the graphite increases very slowly and generates small reactivity feedback.

The second calculated case of UTOP is assumed to be caused by a fuel agglomeration (+200 pcm) sweeping through the core region in about 7 s and returning in another loop time (about 4 s). In the calculation, the flow and inlet temperature have no changes. Figs. 11–13 shows the calculated results.

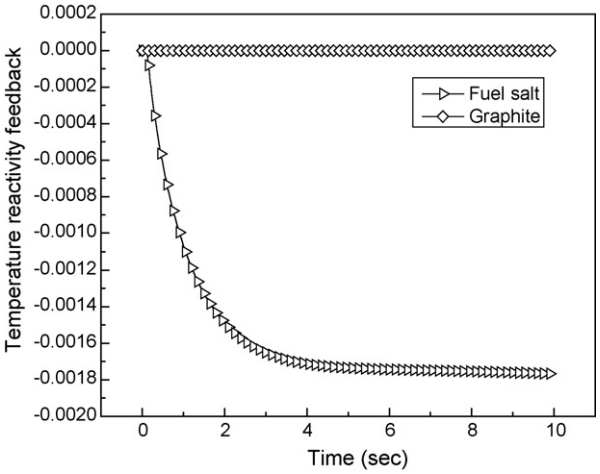

Fig. 10. Temperature reactivity feedback in the UTOP with +200 pcm jump.

From Figs. 11–13, it can be found that the relative power, the average and outlet temperatures of the fuel salt and the reactiv-

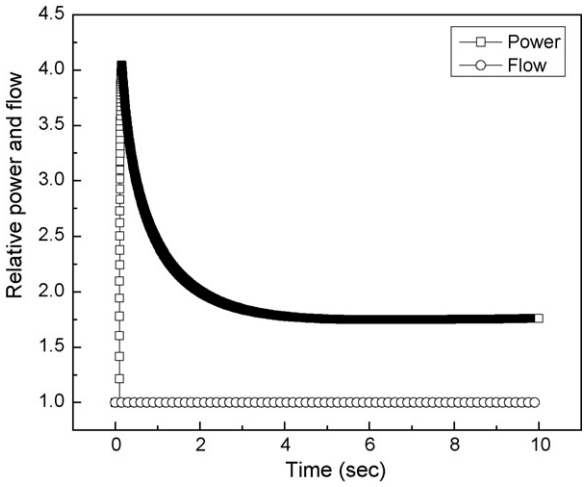

Fig. 8. Relative power and flow in the UTOP with +200 pcm jump.

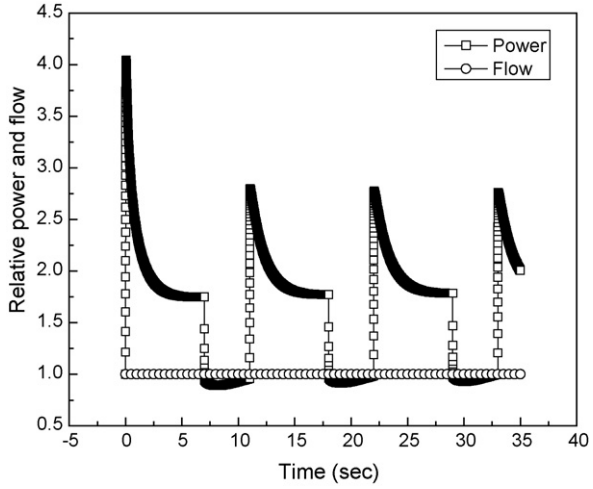

Fig. 11. Relative power and flow in the UTOP with +200 pcm cycle.

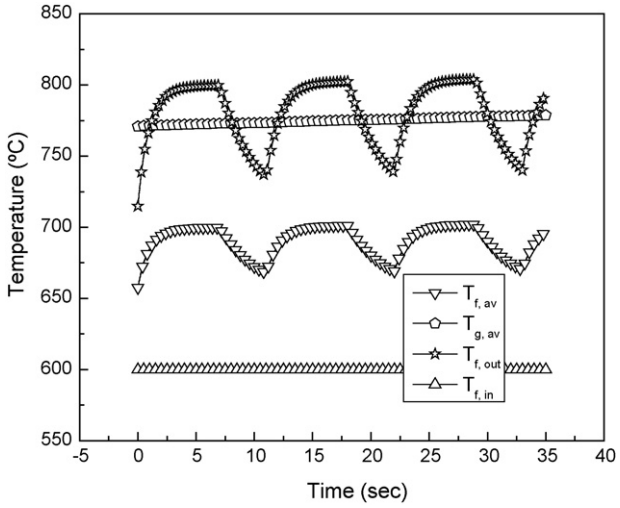

Fig. 12. Temperatures in the UTOP with +200 pcm cycle.

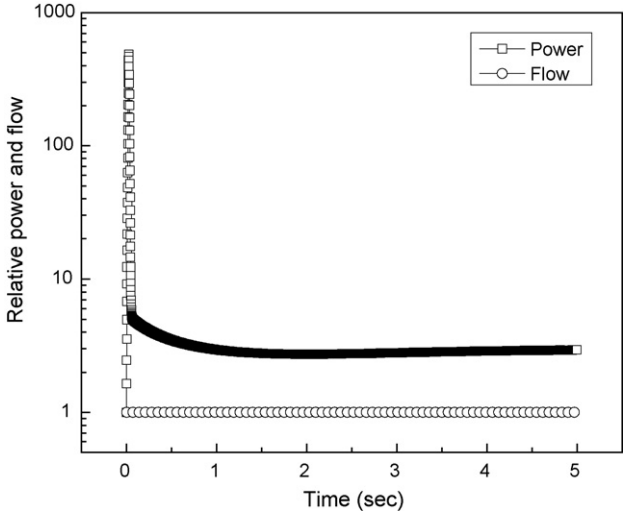

Fig. 14. Relative power and flow in the UTOP with +500 pcm jump.

ity feedback caused by the fuel salt temperatures changing vary periodically, which is corresponding with the cyclical reactivity insertion initiated by the fuel agglomeration cycle. And in every period, the changing trends are similar with those in the first case of UTOP. However, it can be observed that the power peaks following the first power peak are lower, that is because their initial powers are a little lower. Fig. 13 shows that the reactivity feedback caused by the fuel salt is still negative in the loop time, which leads the relative power lower than the rated value in the loop time. In addition, the average temperature of the graphite change little due to its thermal inertia, the reactivity feedback caused by which is nearly zero.

Another two similar cases are also calculated, in which the reactivity of the fuel agglomeration is +500 pcm (about 1.5 dollar). Figs. 14–16 display the results under the condition of +500 pcm reactivity jump, and Figs. 17–19 shows those of +500 pcm reactivity cycle.

From Fig. 14, it can be seen that the insertion of +500 pcm reactivity leads to a power pulse in very short time, the factor of which related to the rated power is nearly 500. The average and outlet temperatures of the fuel salt respond to the power pulse very quickly and increase to 775 °C and 950 °C. The strong negative reactivity feedback generated by the fuel salt makes the relative power decrease and stabilize at about 3, and the average and outlet temperatures of the fuel salt stabilize to 770 °C and 940 °C. In this case,

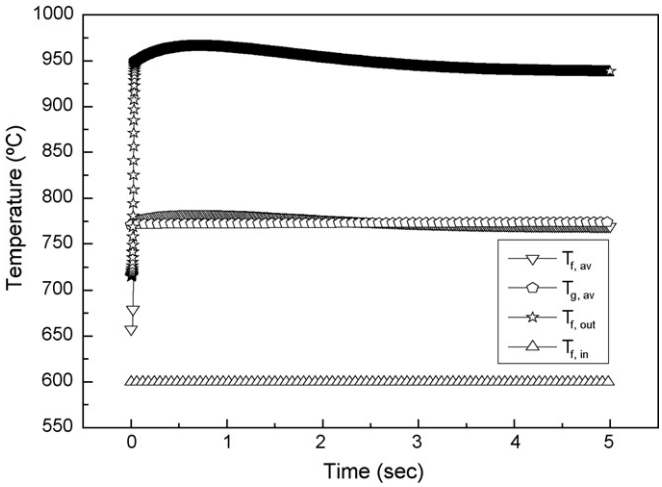

Fig. 15. Temperatures in the UTOP with +500 pcm jump.

the outlet temperature of the fuel salt reaches a maximum value of 970 °C, which is lower than the safety limited value (1400 °C, the boiling temperature of the fuel salt). Similarly with the two cases above, the average temperature of the graphite has little change in this transient condition.

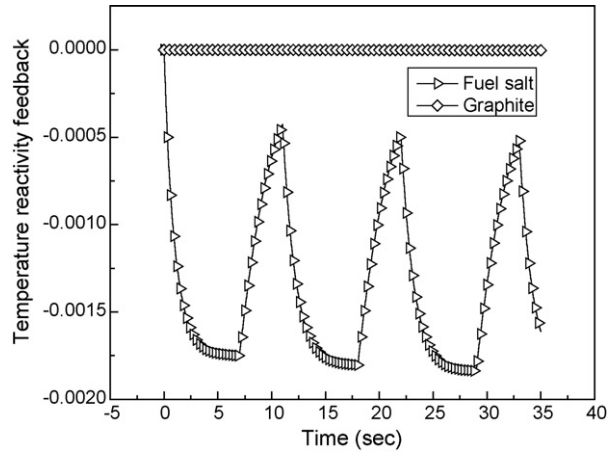

Fig. 13. Temperature reactivity feedback in the UTOP with +200 pcm cycle.

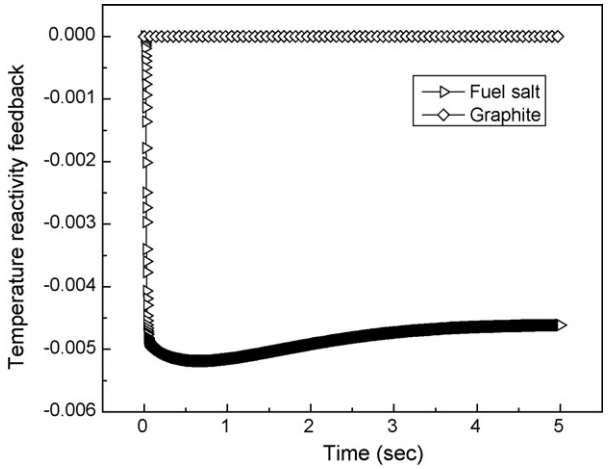

Fig. 16. Temperature reactivity feedback in the UTOP with +500 pcm jump.

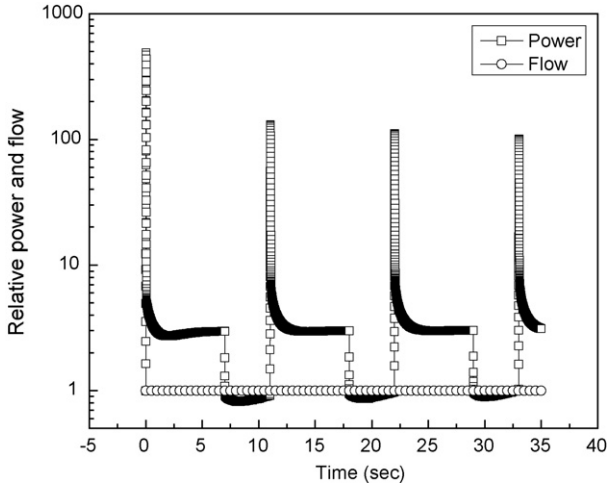

Fig. 17. Relative power and flow in the UTOP with +500 pcm cycle.

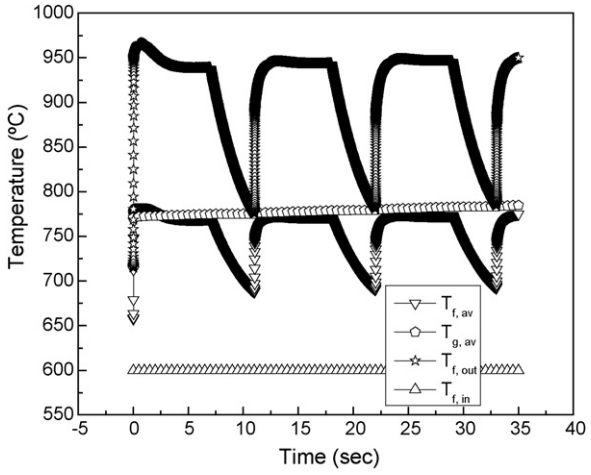

Fig. 18. Temperatures in the UTOP with +500 pcm cycle.

The results of +500 pcm reactivity cycle (as shown in Figs. 17–19) illustrate that the relative power, the average and outlet temperatures of the fuel salt, and the reactivity feedback caused by fuel salt vary periodically, the trends of which in every period are similar with those in the case of +500 pcm jump. The phenomenon that the power peaks following the first one are lower is also observed, and can be interpreted as done in the second case of UTOP.

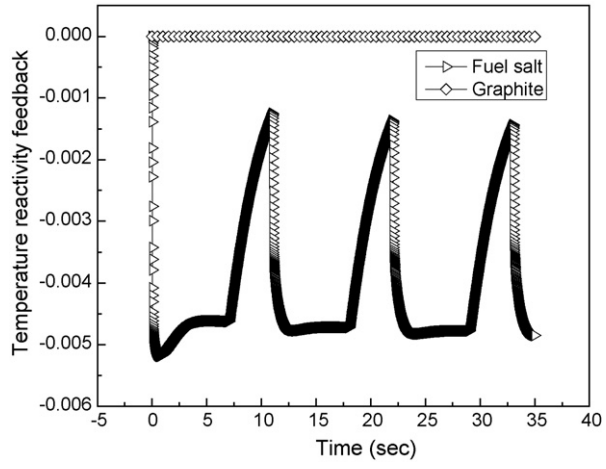

Fig. 19. Temperature reactivity feedback in the UTOP with +500 pcm cycle.

4. Conclusion

In this present research, a general point kinetic model considering the flow effects of the fuel salt is established for the molten salt reactors, and solved by developing a microcomputer code coupling with a simplified heat transfer model in the core. The founded models and developed code are applied to analyze the safety characteristics of the MOSART. Three types of basic transient conditions including the unprotected loss of flow, unprotected overcooling accident and unprotected transient overpower are analyzed. The results show that the MOSART conceptual design is an inherently stable reactor design because of its strong negative reactivity coefficient of the fuel salt temperature in combination with its negative temperature coefficient of the graphite. All calculated transient conditions have no serious challenge to the MOSART even the UTOP with up to 1.5 dollars reactivity insertion. Because of the adoption of modular programming techniques, this code is expected to be applied to transient analysis of other types of molten salt reactors or fluid-fuel reactors.

Acknowledgements

This work is carried out under the financial support of the National Natural Science Foundation of China (Grant No. 10575079). And the authors also wish to acknowledge Dr. W. Maschek, Dr. S. Wang, and Dr. A. Rineiski, of the Institute for Nuclear and Energy Technologies (IKET) of Forschungszentrum Karlsruhe (FZK) for their valuable supports and comments.

References

Bettis, E.S., Schroeder, R.W., Cristy, G.A., et al., 1957. The aircraft reactor experiment—design and construction. Nucl. Sci. Eng. 2, 804–825.
Gear, C.W., 1971. Numerical Initial Value Problems in Ordinary Differential Equation. Prentice-Hall, Englewood Cliffs, pp. 126–187.
Ignatiev, V., Afonichkin, V., Feynberg, O., et al., 2006. Progress in integrated study of molten salt actinide recycler and transmuter system. In: Proc. Ninth Information Exchange Meeting on Actinide and Fission Product Partitioning and Transmutation, France, September 25–29, 2006, Nuclear Energy Agency.
Krepel, J., Grundmann, U., Rohde, U., 2005. DYN1D-MSR dynamics code for molten salt reactors. Ann. Nucl. Energy 32, 1799–1824.
Krepel, J., Grundmann, U., Rohde, U., 2007. DYN3D-MSR spatial dynamics code for molten salt reactors. Ann. Nucl. Energy 34, 449–462.
Maschek, W., Stanculescu, A., Arien, B., et al., 2008. Report on intermediate results of the IAEA CRP on 'Studies of advanced reactor technology options for effective incineration of radioactive waste'. Energy Conver. Manag. 49, 1810–1819.
Merle-Lucotte, E., Heuer, D., Allibert, M., et al., 2008. Optimization and simplification of the concept of non-moderated thorium molten salt reactor. In: Proc. PHYSOR 2008, Interlaken, Switzerland, September 14–19.
Mitachi, K., Yamana, Y., Suzuki, T., Furukawa, K., 1995. Neutronic examination on plutonium transmutation by a small molten-salt fission power station. IAEA-TECDOC-840, 183–193.
MOST Project, 2004. Reactor physics study, design review and nominal operating conditions, non-proliferation issues. Final MOST-Project Report, Brussels.
Rineiski, A., Sinitsa, V., Maschek, W., et al., 2005. Kinetics and cross-section developments for analyses of reactor transmutation concepts with simmer. In: Proc. Mathematics and Computation, Supercomputing, Reactor Physics and Nuclear and Biological Applications, Avignon, France, September 12–15, 2005, American Nuclear Society.
Rosenthal, M.W., Kasten, P.R., Briggs, R.B., 1970. Molten-salt reactors—history, states, and potential. Nucl. Appl. Technol. 8, 107–117.
Shimazu, Y., 1978a. Nuclear safety analysis of a molten salt breeder reactor. J. Nucl. Sci. Technol. 15, 514–522.
Shimazu, Y., 1978b. Locked rotor accident analysis in a molten salt breeder reactor. J. Nucl. Sci. Technol. 15, 935–940.
Suzuki, N., Shimazu, Y., 2006. Preliminary safety analysis on depressurization accident without scram of a molten salt reactor. J. Nucl. Sci. Technol. 43, 720–730.
Suzuki, N., Shimazu, Y., 2008. Reactivity-initiated-accident analysis without scram of a molten salt reactor. J. Nucl. Sci. Technol. 45, 575–581.

Wang, S., Rineiski, A., Maschek, W., 2006. Molten salt related extensions of the SIMMER-III code and its application for a burner reactor. Nucl. Eng. Des. 236, 1580–1588.

Yamamoto, T., Mitachi, K., Suzuki, T., 2005. Steady state analysis of small molten salt reactor (effect of fuel salt flow on reactor characteristics). JSME Int. J. B: Fluids Therm. Eng. 48, 610–617.

Zhang, D.-L., Rineiski, A., Qiu, S.-Z., 2009. Comparison of modeling options for delayed neutron precursor movement in a molten salt reactor. 2009 ANS Annual Meeting, June 14–18, 2009, Atlanta, GA, US, Paper number: 090305.